J|A|C|S ARTICLES

Published on Web 04/22/2009

Polar or Nonpolar? A^+ Cation Polarity Control in $A_2Ti(IO_3)_6$ (A = Li, Na, K, Rb, Cs, Tl)

Hong-Young Chang,† Sang-Hwan Kim,† Kang Min Ok,‡ and P. Shiv Halasyamani*,†

Department of Chemistry, University of Houston, 136 Fleming Building, Houston, Texas 77204-5003, and Department of Chemistry, Chung-Ang University, 221 Heukseok-dong, Dongjak-gu, Seoul 155-756, Republic of Korea

Received February 26, 2009; E-mail: psh@uh.edu

Abstract: We have synthesized a series of new alkali-metal or Tl^+ titanium iodates, $A_2Ti(IO_3)_6$ (A = Li, Na, K, Rb, Cs, Tl). Interestingly the Li and Na phases are noncentrosymmetric (NCS) and polar, whereas the K, Rb, Cs, and Tl analogues are centrosymmetric (CS) and nonpolar. We are able to explain the change from NCS polar to CS nonpolar using cation-size arguments, coordination requirements, and bond valence concepts. The six materials are topologically similar, consisting of TiO_6 octahedra, each of which is bonded to six IO_3 polyhedra. These polyhedral groups are separated by the A^+ cations. Our calculations on $Na_2Ti(IO_3)_6$ indicate that polarization reversal is energetically very unfavorable, rendering the material polar but *not* ferroelectric. For all of the materials, synthesis, structural characterization, electronic structure analysis, infrared spectra, UV−vis and thermogravimetric measurements, and ion-exchange reactions are reported. For the polar materials, second-harmonic generation, piezoelectricity, and polarization measurements were performed. Crystal data: $Li_2Ti(IO_3)_6$: hexagonal, space group $P6_3$ (No. 173), $a = b = 9.3834(11)$ Å, $c = 5.1183(6)$ Å, $Z = 1$. $Na_2Ti(IO_3)_6$: hexagonal, space group $P6_3$ (No. 173), $a = b = 9.649(3)$ Å, $c = 5.198(3)$ Å, $Z = 1$. $K_2Ti(IO_3)_6$: trigonal, space group $R\bar{3}$ (No. 148), $a = b = 11.2703(6)$ Å, $c = 11.3514(11)$ Å, $Z = 3$. $Rb_2Ti(IO_3)_6$: trigonal, space group $R\bar{3}$ (No. 148), $a = b = 11.3757(16)$ Å, $c = 11.426(3)$ Å, $Z = 3$. $Cs_2Ti(IO_3)_6$: trigonal, space group $R\bar{3}$ (No. 148), $a = b = 11.6726(5)$ Å, $c = 11.6399(10)$ Å, $Z = 3$. $Tl_2Ti(IO_3)_6$: trigonal, space group $R\bar{3}$ (No. 148), $a = b = 11.4167(6)$ Å, $c = 11.3953(11)$ Å, $Z = 3$.

Introduction

Polarity, or the occurrence of a dipole moment, is of broad and current interest attributable to a variety of important technological properties, such as pyroelectricity and ferroelectricity.[1,2] The concept of polarity is straightforward in molecular compounds such as H_2O, NH_3, and CO. In the solid state, however, a material is considered polar only if it is found in one of ten polar crystal classes: 1, 2, 3, 4, 6, *m*, *mm*2, 3*m*, 4*mm*, or 6*mm*.[3] Additionally, specifically defined polar directions have been designated for each polar crystal class.[3] Interest in polarity and polar materials stems from two technologically important properties: pyroelectricity and ferroelectricity. For either to occur, the material in question must be polar. With pyroelectricity, a change in the magnitude of the polarization (dipole moment) with respect to temperature is observed, whereas with ferroelectricity, the dipole moment may be reversed in the presence of an external electric field. In pyroelectrics, this dipole moment reversibility is not observed. Thus, all ferroelectrics are pyroelectrics, but the converse is not true. However, the challenge of synthesizing a new solid-state polar material remains. Poeppelmeier and co-workers[4−8] have synthesized and examined the crystallographically ordered transition-metal oxyfluorides $[MO_xF_{6-x}]^{n-}$ (M = d^0 transition metal, x = 1–3, and n = 2, 3) and determined that changes to the bond network lead to different crystal symmetries: polar or nonpolar. We have focused on synthesizing new polar oxide materials that contain second-order Jahn−Teller (SOJT)-distorted cations,[9−15] i.e., octahedrally coordinated d^0 transition-metal ions (Ti^{4+}, Nb^{5+}, W^{6+}, etc.) and lone-pair cations (Se^{4+}, Te^{4+}, Tl^+, etc.).[16−27] In oxides, both groups of cations are in asymmetric, polar

† University of Houston.
‡ Chung-Ang University.

(1) Lang, S. B.; Das-Gupta, D. K. In *Handbook of Advanced Electronic and Photonic Materials and Devices*; Nalwa, H. S., Ed.; Academic Press: San Francisco, 2001; Vol. 4, pp 1−55.
(2) Lines, M. E.; Glass, A. M. *Principles and Applications of Ferroelectrics and Related Materials*; Oxford University Press: Oxford, U.K., 1991.
(3) Hahn, T. *International Tables for Crystallography, Volume A: Space Group Symmetry*; Kluwer Academic: Dordrecht, The Netherlands, 2006.
(4) Maggard, P. A.; Stern, C. L.; Poeppelmeier, K. R. *J. Am. Chem. Soc.* **2001**, *123*, 7742.
(5) Welk, M. E.; Norquist, A.; Arnold, F. P.; Stern, C. L.; Poeppelmeier, K. R. *Inorg. Chem.* **2002**, *41*, 5119.
(6) Maggard, P. A.; Nault, T. S.; Stern, C. L.; Poeppelmeier, K. R. *J. Solid State Chem.* **2003**, *175*, 27.
(7) Izumi, H. K.; Kirsch, J. E.; Stern, C. L.; Poeppelmeier, K. R. *Inorg. Chem.* **2005**, *44*, 884.
(8) Marvel, M. R.; Lesage, J.; Baek, J.; Halasyamani, P. S.; Stern, C. L.; Poeppelmeier, K. R. *J. Am. Chem. Soc.* **2007**, *129*, 13963.
(9) Opik, U.; Pryce, M. H. L. *Proc. R. Soc. London, Ser. A* **1957**, *238*, 425.
(10) Bader, R. F. W. *Mol. Phys.* **1960**, *3*, 137.
(11) Bader, R. F. W. *Can. J. Chem.* **1962**, *40*, 1164.
(12) Pearson, R. G. *J. Am. Chem. Soc.* **1969**, *91*, 4947.
(13) Pearson, R. G. *THEOCHEM* **1983**, *103*, 25.
(14) Wheeler, R. A.; Whangbo, M. H.; Hughbanks, T.; Hoffmann, R.; Burdett, J. K.; Albright, T. A. *J. Am. Chem. Soc.* **1986**, *108*, 2222.
(15) Goodenough, J. B. *Annu. Rev. Mater. Sci.* **1998**, *28*, 1.
(16) Halasyamani, P. S.; Poeppelmeier, K. R. *Chem. Mater.* **1998**, *10*, 2753.

coordination environments. With the d^0 metal ions, an out-of-center displacement is observed,[15] whereas with the lone-pair cations, a nonbonded electron pair is found.[28−31] In both groups, the local site symmetry of the cation is changed from centrosymmetric (CS) and nonpolar to noncentrosymmetric (NCS) and polar. We suggest that incorporating locally polar polyhedra into a solid-state framework may result in a macroscopically polar material.[26,27,32] In order to better understand the structural basis of the polarity and to predict when macroscopic polarity will occur, it is necessary to examine the bond network, i.e., the interactions between the asymmetric polyhedra and the framework cations.

We have synthesized a series of new alkali-metal or thallium titanium iodates with the stoichiometry $A_2Ti(IO_3)_6$ (A = Li, Na, K, Rb, Cs, Tl). A communication regarding $Li_2Ti(IO_3)_6$ has recently appeared.[32] All six materials exhibit a "zero-dimensional" crystal structure consisting of a TiO_6 octahedron linked to six IO_3 polyhedra. Between these polyhedra are the alkali-metal or thallium cations. Interestingly, $Li_2Ti(IO_3)_6$ and $Na_2Ti(IO_3)_6$ are NCS polar and isostructural, whereas $A_2Ti(IO_3)_6$ (A = K, Rb, Cs, Tl) are CS nonpolar and isostructural. Using cation size arguments, coordination preferences, and bond valence concepts, we will demonstrate that it is the "A" cation that controls the macroscopic polarity of the reported materials. In addition, electronic structure calculations indicate that although $Na_2Ti(IO_3)_6$ is polar, macroscopic dipole moment reversibility is energetically very unfavorable, and thus, the material is *not* ferroelectric. We also describe in this paper the synthesis, structure, characterization, and calculations on $A_2Ti(IO_3)_6$ (A = Li, Na, K, Rb, Cs, Tl).

Experimental Section

Reagents. Na_2CO_3 (Alfa Aesar, 99%), K_2CO_3 (Alfa Aesar, 99%), Rb_2CO_3 (Alfa Aesar, 99%), Cs_2CO_3 (Alfa Aesar, 99.5%), Tl_2CO_3 (Alfa Aesar, 99%), HIO_3 (Alfa Aesar, 99%), and TiO_2 (Aldrich, 99%) were used as received.

Synthesis. The synthesis of $Li_2Ti(IO_3)_6$ has been reported.[32] For $Na_2Ti(IO_3)_6$, 0.50 g (4.7 mmol) of Na_2CO_3, 0.30 g (3.8 mmol) of TiO_2, and 5.0 g (28 mmol) of HIO_3 were combined with 10 mL of H_2O. For $K_2Ti(IO_3)_6$, 0.23 g (1.7 mmol) of K_2CO_3, 0.10 g (1.3 mmol) of TiO_2, and 3.0 g (17 mmol) of HIO_3 were combined with 10 mL of H_2O. For $Rb_2Ti(IO_3)_6$, 0.35 g (1.7 mmol) of Rb_2CO_3, 0.10 g (1.3 mmol) of TiO_2, and 3.0 g (17 mmol) of HIO_3 were combined with 10 mL of H_2O. For $Cs_2Ti(IO_3)_6$, 0.27 g (1.4 mmol) of Cs_2CO_3, 0.10 g (1.3 mmol) of TiO_2, and 3.0 g (17 mmol) of HIO_3 were combined with 10 mL of H_2O. For $Tl_2Ti(IO_3)_6$, 0.65 g (1.4 mmol) of Tl_2CO_3, 0.10 g (1.3 mmol) of TiO_2, and 5.0 g (28 mmol) of HIO_3 were combined with 10 mL of H_2O. The respective solutions were placed in 23 mL Teflon-lined autoclaves that were subsequently sealed. The autoclaves were gradually heated to 230 °C, held there for 4 days, and cooled slowly to room temperature at a rate of 6 °C/h. The mother liquor was decanted from the products, which were recovered by filtration and washed with distilled water, ethanol, and acetone. Colorless crystals, the only product from each reaction, were obtained in ∼80−90% yield based on TiO_2 for $A_2Ti(IO_3)_6$ (A = Na, K, Rb, Cs, Tl).

Single-Crystal X-ray Diffraction. Colorless needle-shaped 0.01 × 0.02 × 0.05 mm^3, cube-shaped 0.01 × 0.01 × 0.01 mm^3 and 0.10 × 0.10 × 0.10 mm^3, and block-shaped 0.10 × 0.10 × 0.20 mm^3 and 0.01 × 0.01 × 0.02 mm^3 crystals of $Na_2Ti(IO_3)_6$, $K_2Ti(IO_3)_6$, $Rb_2Ti(IO_3)_6$, $Cs_2Ti(IO_3)_6$, and $Tl_2Ti(IO_3)_6$, respectively, were used for single-crystal X-ray diffraction (XRD) data collection. The data were collected using a Siemens SMART APEX diffractometer equipped with a 1K CCD area detector using graphite-monochromatized Mo Kα radiation. A hemisphere of data was collected using a narrow-frame method with scan widths of 0.30° in ω and an exposure time of 50−60 s per frame. The data were integrated using the Siemens SAINT program,[33] and the intensities were corrected for Lorentz polarization, air absorption, and absorption attributable to the variation in the path length through the detector face plate. Psi scans were used for the absorption correction to the data. The data were solved by direct methods and refined against F^2 by full-matrix least-squares techniques using SHELXS-97 and SHELXL-97, respectively.[34−36] All of the atoms in each structure were refined with anisotropic thermal parameters and the refinements converged for $I > 2\sigma(I)$. For $Na_2Ti(IO_3)_6$, the Ti^{4+} is disordered over two sites. A fractional occupancy of 0.5 was set for the Ti^{4+} cation. Also, for $Na_2Ti(IO_3)_6$ the Flack parameter was refined to 0.08(9). All of the structures were checked for missing symmetry elements using PLATON.[37] Relevant crystallographic data and selected bond distances for $Li_2Ti(IO_3)_6$, $Na_2Ti(IO_3)_6$, $K_2Ti(IO_3)_6$, $Rb_2Ti(IO_3)_6$, $Cs_2Ti(IO_3)_6$, and $Tl_2Ti(IO_3)_6$ are given in Tables 1 and 2, respectively, and additional details such as atomic coordinates and thermal parameters are provided in the Supporting Information.

Powder X-ray Diffraction. Powder XRD data were collected using a PANalytical X'Pert PRO diffractometer with Cu Kα radiation. The 2θ range was 5−60° with a step size of 0.008° and a fixed time of 0.2 s. The powder XRD patterns for $Na_2Ti(IO_3)_6$, $K_2Ti(IO_3)_6$, $Rb_2Ti(IO_3)_6$, $Cs_2Ti(IO_3)_6$, and $Tl_2Ti(IO_3)_6$, showed good agreement with the calculated XRD patterns from the single-crystal models (see the Supporting Information).

Infrared Spectroscopy. IR spectra were recorded on a Mattson FTIR 5000 spectrometer in the 400−4000 cm^{-1} range.

UV−Vis Diffuse Reflectance Spectroscopy. UV−vis reflectance data were collected on a Varian Cary 500 Scan UV−vis−NIR spectrophotometer over the spectral range 200−1500 nm at room temperature. Poly(tetrafluoroethylene) was used as a reference material. Reflectance spectra were converted to absorbance using the Kubelka−Munk function.[38,39]

(17) Ok, K. M.; Bhuvanesh, N. S. P.; Halasyamani, P. S. *J. Solid State Chem.* **2001**, *161*, 57.
(18) Goodey, J.; Broussard, J.; Halasyamani, P. S. *Chem. Mater.* **2002**, *14*, 3174.
(19) Goodey, J.; Ok, K. M.; Broussard, J.; Hofmann, C.; Escobedo, F. V.; Halasyamani, P. S. *J. Solid State Chem.* **2003**, *175*, 3.
(20) Ra, H. S.; Ok, K. M.; Halasyamani, P. S. *J. Am. Chem. Soc.* **2003**, *125*, 7764.
(21) Chi, E. O.; Gandini, A.; Ok, K. M.; Zhang, L.; Halasyamani, P. S. *Chem. Mater.* **2004**, *16*, 3616.
(22) Ok, K. M.; Halasyamani, P. S. *Angew. Chem., Int. Ed.* **2004**, *43*, 5489.
(23) Ok, K. M.; Halasyamani, P. S. *Inorg. Chem.* **2005**, *44*, 9353.
(24) Chi, E. O.; Ok, K. M.; Porter, Y.; Halasyamani, P. S. *Chem. Mater.* **2006**, *18*, 2070.
(25) Sivakumar, T.; Chang, H. Y.; Baek, J.; Halasyamani, P. S. *Chem. Mater.* **2007**, *19*, 4710.
(26) Chang, H. Y.; Sivakumar, T.; Ok, K. M.; Halasyamani, P. S. *Inorg. Chem.* **2008**, *47*, 8511.
(27) Kim, J.-H.; Baek, J.; Halasyamani, P. S. *Chem. Mater.* **2008**, *20*, 3542.
(28) Gillespie, R. J.; Nyholm, R. S. *Q. Rev., Chem. Soc.* **1957**, *11*, 339.
(29) Orgel, L. E. *J. Chem. Soc* **1959**, 3815.
(30) Seshadri, R.; Hill, N. A. *Chem. Mater.* **2001**, *13*, 2892.
(31) Stoltzfus, M. W.; Woodward, P.; Seshadri, R.; Park, J.-H.; Bursten, B. *Inorg. Chem.* **2007**, *46*, 3839.
(32) Chang, H. Y.; Kim, S.-H.; Halasyamani, P. S.; Ok, K. M. *J. Am. Chem. Soc.* **2009**, *131*, 2426.
(33) *SAINT: A Program for Area Detector Absorption Correction*, version 4.05; Siemens Analytical X-ray Systems, Inc.: Madison, WI, 1995.
(34) Sheldrick, G. M. *SHELXS-97: A Program for Automatic Solution of Crystal Structures*; University of Göttingen: Göttingen, Germany, 1997.
(35) Sheldrick, G. M. *SHELXL-97: A Program for Crystal Structure Refinement*; University of Göttingen: Göttingen, Germany, 1997.
(36) Sheldrick, G. M. *SHELXTL DOS/Windows/NT*, version 5.10; Bruker Analytical X-Ray Instruments, Inc.: Madison, WI, 1997.
(37) Spek, A. L. *PLATON*; Utrecht University: Utrecht, The Netherlands, 2001.
(38) Kubelka, P.; Munk, F. Z. *Tech. Phys.* **1931**, *12*, 593.

Table 1. Crystallographic Data for $A_2Ti(IO_3)_6$ (A = Li, Na, K, Rb, Cs, Tl)

formula	$Li_2Ti(IO_3)_6$[a]	$Na_2Ti(IO_3)_6$	$K_2Ti(IO_3)_6$	$Rb_2Ti(IO_3)_6$	$Cs_2Ti(IO_3)_6$	$Tl_2Ti(IO_3)_6$
fw	1111.18	1143.28	1175.50	1268.24	1363.12	1506.04
T (K)	296.0(2)	296.0(2)	296.0(2)	296.0(2)	296.0(2)	296.0(2)
λ (Å)	0.71073	0.71073	0.71073	0.71073	0.71073	0.71073
crystal system	hexagonal	hexagonal	trigonal	trigonal	trigonal	trigonal
space group	$P6_3$ (No. 173)	$P6_3$ (No. 173)	$R\bar{3}$ (No. 148)	$R\bar{3}$ (No. 148)	$R\bar{3}$ (No. 148)	$R\bar{3}$ (No. 148)
a (Å)	9.3834(11)	9.649(3)	11.2703(6)	11.3757(16)	11.6726(5)	11.4167(6)
c (Å)	5.1183(6)	5.198(3)	11.3514(11)	11.426(3)	11.6399(10)	11.3953(11)
α (deg)	90	90	90	90	90	90
γ (deg)	120	120	120	120	120	120
V (Å^3)	390.28(8)	419.1(3)	1248.68(15)	1280.5(4)	1373.46(14)	1286.29(16)
Z	1	1	3	3	3	3
ρ_{calcd} (g/cm^3)	4.728	4.530	4.690	4.934	4.944	5.833
μ (mm^{-1})	12.511	11.705	12.235	17.108	14.588	30.092
$2\theta_{max}$ (deg)	57.78	54.86	57.40	50.92	57.94	57.86
R_{int}	0.0598	0.0539	0.0163	0.0322	0.0306	0.0330
GOF(F^2)	1.226	1.099	1.152	1.137	0.907	1.162
$R(F)$[b]	0.0301	0.0354	0.0223	0.0456	0.0164	0.0421
$R_w(F_o^2)$[c]	0.0563	0.0553	0.0517	0.1198	0.0274	0.1133
Flack param.	0.05(9)	0.08(9)	N/A	N/A	N/A	N/A

[a] Data from ref 32. [b] $R(F) = \sum||F_o| - |F_c||/\sum|F_o|$. [c] $R_w(F_o^2) = [\sum w(F_o^2 - F_c^2)^2/\sum w(F_o^2)^2]^{1/2}$.

Table 2. Selected Bond Distances (Å) in $A_2Ti(IO_3)_6$ (A = Li, Na, K, Rb, Cs, Tl)

bond	$Li_2Ti(IO_3)_6$	$Na_2Ti(IO_3)_6$
A(1)−O(2) × 3	2.114(14)	2.389(8)
A(1)−O(3) × 3	2.222(14)	2.314(8)
Ti(1)−O(1) × 3	2.028(7)	2.041(9)
Ti(1)−O(1) × 3	2.052(7)	2.056(9)
I(1)−O(1)	1.871(6)	1.880(7)
I(1)−O(2)	1.791(5)	1.786(7)
I(1)−O(3)	1.799(5)	1.776(7)

bond	$K_2Ti(IO_3)_6$	$Rb_2Ti(IO_3)_6$	$Cs_2Ti(IO_3)_6$	$Tl_2Ti(IO_3)_6$
A(1)−O(1) × 3	3.070(5)	3.116(13)	3.135(3)	3.062(10)
A(1)−O(2) × 3	2.795(5)	2.873(15)	3.108(3)	2.917(10)
A(1)−O(3) × 3	2.914(4)	2.971(13)	3.177(3)	3.000(10)
Ti(1)−O(1) × 6	1.944(4)	1.949(12)	1.943(3)	1.930(10)
I(1)−O(1)	1.869(4)	1.861(12)	1.856(2)	1.871(10)
I(1)−O(2)	1.808(4)	1.800(13)	1.798(3)	1.814(10)
I(1)−O(3)	1.793(4)	1.791(12)	1.786(3)	1.792(10)

Thermogravimetric Analysis. Thermogravimetric analysis (TGA) was peformed using a TGA 951 thermogravimetric analyzer (TA Instruments). The samples were placed in a platinum crucible and heated at a rate of 10 °C/min from room temperature to 800 °C under flowing nitrogen.

Ion-Exchange Reactions. A sample (~0.1 g) of each of the reported materials $A_2Ti(IO_3)_6$ was added to 6 mL of 2 M ACl (A = Li, Na, K, Rb, Cs). Each mixture was stirred at room temperature for 24 h or at 60 °C for 12 h. In each instance, the white powder that was recovered was washed with distilled water, after which powder XRD was performed.

Second-Harmonic Generation. Powder second-harmonic generation (SHG) measurements were performed on a modified Kurtz-NLO[40] system using a pulsed Nd:YAG laser with a wavelength of 1064 nm. A detailed description of the equipment and methodology has been published.[41] SHG efficiency has been shown to depend strongly on particle size, and thus, polycrystalline samples were ground and sieved into distinct particle size ranges (20−45, 45−63, 63−75, 75−90, and >90 μm). In order to make relevant comparisons with known SHG materials, crystalline α-SiO_2 and $LiNbO_3$ were also ground and sieved into the same particle size ranges. No index matching fluid was used in any of the experiments.

Piezoelectric Measurements. Converse piezoelectric measurements were performed using a Radiant Technologies RT66A piezoelectric test system with a TREK (model 609E-6) high-voltage amplifier, Precision Materials Analyzer, Precision High-Voltage Interface, and MTI 2000 Fotonic Sensor. $Na_2Ti(IO_3)_6$ was pressed into 12 mm diameter, ~0.5 mm thick pellets and sintered at 300 °C for 6 h. Silver paste was applied to both sides as electrodes and cured at 200 °C for 3 h. A maximum voltage of 500 V was applied to the sample.

Polarization Measurements. The polarization was measured on a Radiant Technologies RT66A ferroelectric test system with a TREK high-voltage amplifier between room temperature and 165 °C in a Delta 9023 environmental test chamber. The unclamped pyroelectric coefficient, defined as dP/dT [i.e., the change in the polarization (P) with respect to the change in temperature (T)] was determined by measuring the polarization as a function of temperature. A detailed description of the methodology used has been published elsewhere.[41] $Na_2Ti(IO_3)_6$ was pressed into ~12 mm diameter, ~1 mm thick pellets and sintered at 300 °C (well below the decomposition temperatures) for 6 h. Silver paste was applied to both sides as electrodes and cured at 200 °C for 3 h. To determine the ferroelectric behavior, polarization measurements were done at room temperature under a static electric field of 13.5 kV/cm at frequencies ranging from 5 to 200 Hz. For the pyroelectric measurements, the polarization was measured statically from room temperature to 165 °C in 20 °C increments, with an electric field of 11 kV/cm. The temperature was allowed to stabilize before the polarization was measured.

Electronic Structure Calculations. First-principles electronic band structures for NCS polar $Na_2Ti(IO_3)_6$ and CS nonpolar $K_2Ti(IO_3)_6$ and $Tl_2Ti(IO_3)_6$ were carried out using plane-wave pseudopotential calculations as implemented in the Quantum ESPRESSO (version 4.0.1) package.[42] Norm-conserving Martins−Troullier (MT) pseudopotentials[43] were utilized with the local density approximation[44,45] and the generalized gradient approximation[46] for the exchange-correlation corrections. Pseudopotentials generated from the Fritz Haber Institute (FHI) code were converted for the calculations. The plane-wave energy cutoff was set to 37

(39) Tauc, J. *Mater. Res. Bull.* **1970**, *5*, 721.
(40) Kurtz, S. K.; Perry, T. T. *J. Appl. Phys.* **1968**, *39*, 3798.
(41) Ok, K. M.; Chi, E. O.; Halasyamani, P. S. *Chem. Soc. Rev.* **2006**, *35*, 710.
(42) Baroni, S.; Dal Corso, A.; de Gironcoli, S.; Giannozzi, P.; Cavazzoni, C.; Ballabio, G.; Scandolo, S.; Chiarotti, G.; Focher, P.; Pasquarello, A.; Laasonen, K.; Trave, A.; Car, R.; Marzari, N.; Kokalj, A. http://www.quantum-espresso.org/ (accessed April 13, 2009).
(43) Troullier, N.; Martins, J. L. *Phys. Rev. B* **1991**, *43*, 1993.
(44) Ceperley, D. M.; Alder, B. J. *Phys. Rev. Lett.* **1980**, *45*, 566.
(45) Perdew, J. P.; Zunger, A. *Phys. Rev. B* **1981**, *23*, 5048.
(46) Perdew, J. P.; Burke, K.; Ernzerhof, M. *Phys. Rev. Lett.* **1996**, *77*, 3865.

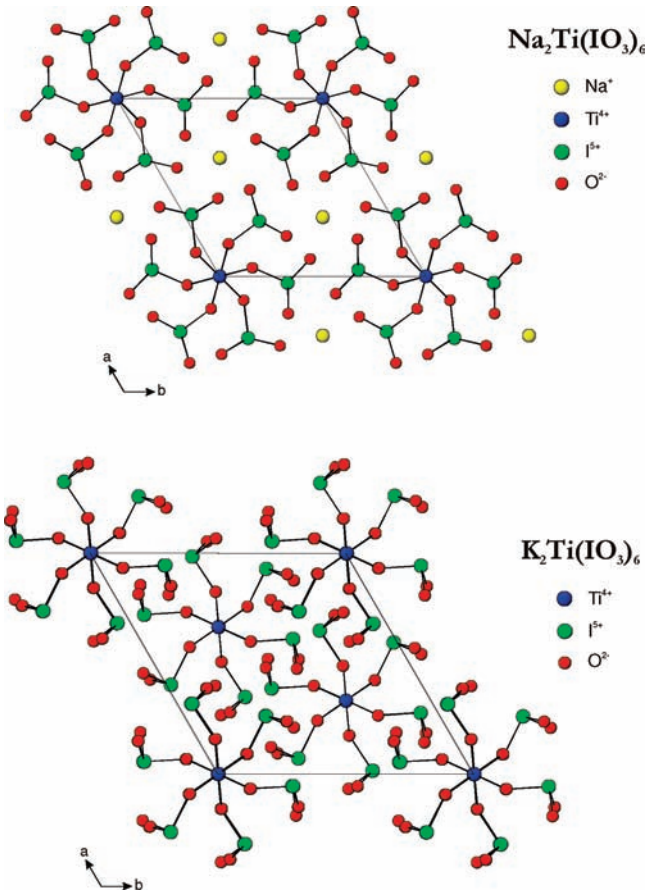

Figure 1. Ball-and-stick representations of (top) $Na_2Ti(IO_3)_6$ and (bottom) $K_2Ti(IO_3)_6$. In the bottom figure, the K^+ ions have been removed for clarity.

Ry. We used **k**-point grids of 5 × 5 × 9 for $Na_2Ti(IO_3)_6$ and 3 × 3 × 3 for $K_2Ti(IO_3)_6$ and $Tl_2Ti(IO_3)_6$ for Brillouin zone integrations. The total-energy convergence threshold was set to 10^{-6} Ry. For the $Na_2Ti(IO_3)_6$ calculations, a disorder-free structure was adopted by lowering the symmetry to space group *P*3 (No. 143). The *P*3 model has the vacancy and the Ti^{4+} cation alternating in an ordered manner along the *c* direction.[32]

Results and Discussion

Structures. Although the six materials are stoichiometrically identical, $Li_2Ti(IO_3)_6$ and $Na_2Ti(IO_3)_6$ are NCS polar, whereas $A_2Ti(IO_3)_6$ (A = K, Rb, Cs, Tl) are CS nonpolar. We will discuss the NCS polar vs CS nonpolar difference in more detail later in the paper. All six materials exhibit a zero-dimensional structure consisting of a TiO_6 octahedron that is linked to six IO_3 polyhedra. The groups of TiO_6 and IO_3 polyhedra are separated by alkali-metal or Tl^+ cations (see Figure 1). With $Li_2Ti(IO_3)_6$ and $Na_2Ti(IO_3)_6$, the Ti^{4+} cation is disordered over two sites, with a set occupancy of 50% on each site, whereas Ti^{4+} is not disordered in the remaining four materials. Full occupation of Ti^{4+} would create a one-dimensional structure but would result in Ti−Ti interactions of ∼2.6 Å. These interactions are extremely unlikely since $A_2Ti(IO_3)_6$ (A = Li, Na) are colorless and insulating. We speculate that ordering at low temperatures is possible, assuming a change in symmetry. All of the structures may be written in connectivity terms as $\{[TiO_{6/2}]^{2-}\cdot 6[IO_{1/2}O_{2/1}]^0\}^{2-}$, with charge balance maintained by two alkali or Tl^+ cations. The Li^+ and Na^+ cations are in sixfold pseudo-octahedral coordination environments with bond distances in the range 2.114(14)−2.389(8) Å, whereas the K^+, Rb^+, Cs^+, and Tl^+ cations are in ninefold coordination environments with bond distances in the range 2.795(5)−3.177(3) Å. The Ti−O and I−O bond distances range from 1.930(10) to 2.056(9) and 1.776(7) to 1.880(7) Å, respectively (see Table 2). In $Li_2Ti(IO_3)_6$ and $Na_2Ti(IO_3)_6$, the Ti^{4+} cations are slightly displaced toward one face of their oxide octahedron (C_3-type distortion), resulting in three "short" [2.028(7) Å × 3 and 2.041(9) Å × 3, respectively] and three "long" [2.052(7) Å × 3 and 2.056(9) Å × 3, respectively] Ti−O bonds. In $A_2Ti(IO_3)_6$ (A = K, Rb, Cs, Tl), the Ti^{4+} cations are in the center of their oxide octahedra with one unique Ti−O bond distance of ∼1.94 Å. Each I^{5+} cation is bonded to three oxygen atoms in a trigonal pyramidal coordination environment as a result of its stereoactive lone pair. In $Li_2Ti(IO_3)_6$ and $Na_2Ti(IO_3)_6$, all of the lone pairs on the I^{5+} cations are aligned in a parallel manner, producing a macroscopic dipole moment and thereby creating a polar material (see Figure 2). In $A_2Ti(IO_3)_6$ (A = K, Rb, Cs, Tl), the lone pairs on IO_3 polyhedra located trans to each other are oriented in opposite directions (see Figure 3); this results in cancellation of the local dipole moments, rendering the materials nonpolar. It is of interest to note that $K_2Ti(IO_3)_6$, $Rb_2Ti(IO_3)_6$, $Cs_2Ti(IO_3)_6$, and $Tl_2Ti(IO_3)_6$ are isostructural, as the coordination environments of K^+, Rb^+, Cs^+, and Tl^+ are similar (see Figures S3−S6 in the Supporting Information). These similar coordination environments indicate that the lone pair on Tl^+ is inert rather than stereoactive. Our electronic structure calculations are consistent with this observation (see Figure 3 and Calculations section). The inertness of the Tl^+ lone pair in $Tl_2Ti(IO_3)_6$ is in contrast to the stereoactive nature that has been observed previously in other Tl^+ materials.[47,48]

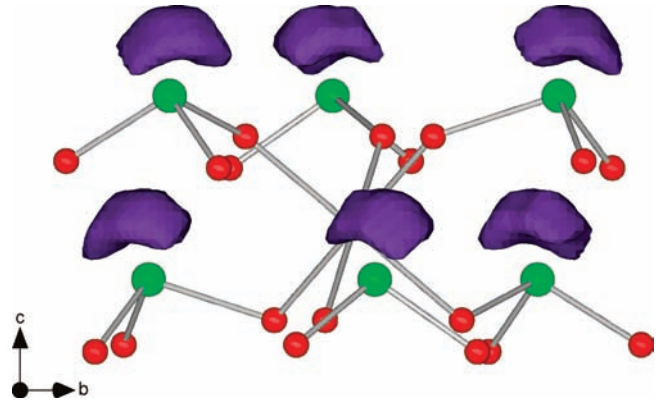

Figure 2. Visualization of the stereoactive lone pairs (purple) using ELFs for $Na_2Ti(IO_3)_6$ with $\eta = 0.9$, as obtained from pseudopotential calculations. I, green; O, red. It should be noted that all of the lone pairs are aligned in a parallel manner.

Bond valence sum (BVS) calculations[49,50] resulted in values of 0.91−1.21, 3.97−4.23, and 4.86−5.09 for the alkali-metal ion or Tl^+, Ti^{4+}, and I^{5+}, respectively. Two structural parameters that incorporate bond valence concepts are the bond strain index (BSI)[51] and global instability index (GII).[52] Large BSI and GII values are indicative of electronic and lattice-induced strains,

(47) Mudring, A.-V. *Eur. J. Inorg. Chem.* **2007**, 882.
(48) Rieger, F.; Mudring, A.-V. *Inorg. Chem.* **2007**, *46*, 446.
(49) Brown, I. D.; Altermatt, D. *Acta Crystallogr.* **1985**, *B41*, 244.
(50) Brese, N. E.; Okeeffe, M. *Acta Crystallogr.* **1991**, *B47*, 192.
(51) Preiser, C.; Losel, J.; Brown, I. D.; Kunz, M.; Skowron, A. *Acta Crystallogr.* **1999**, *B55*, 698.
(52) Salinas-Sanchez, A.; Garcia-Munoz, J. L.; Rodriguez-Carvajal, J.; Saez-Puche, R.; Martinez, J. L. *J. Solid State Chem.* **1992**, *100*, 210.

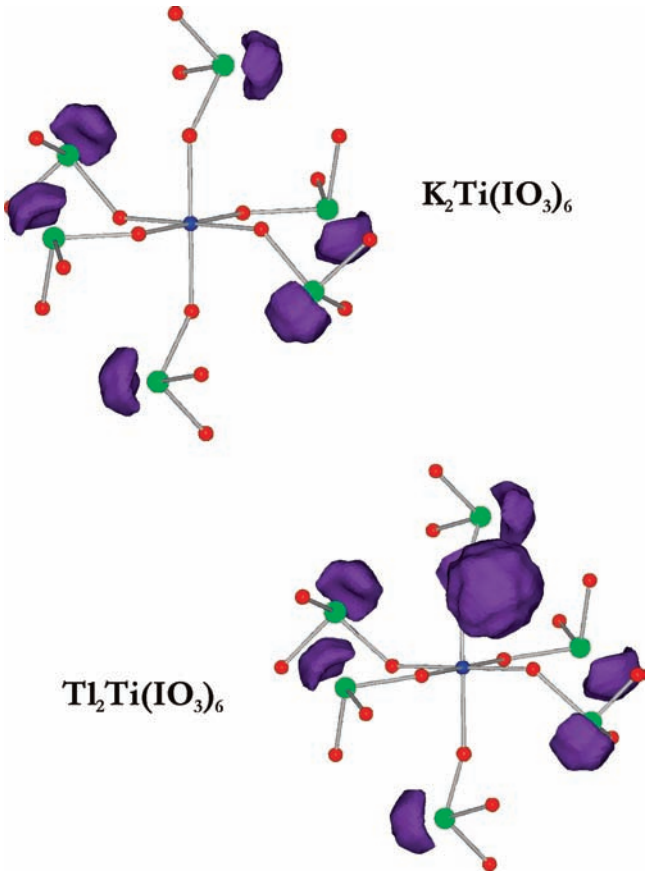

Figure 3. Visualization of the stereoactive lone pairs (purple) through ELFs for (top) $K_2Ti(IO_3)_6$ and (bottom) $Tl_2Ti(IO_3)_6$ with $\eta = 0.9$, as obtained from pseudopotential calculations. Ti, blue; I, green; O, red. It should be noted that the lone pairs in each material are aligned in opposite directions. In the $Tl_2Ti(IO_3)_6$ figure, the electron density around Tl^+ is spherical, indicating that the lone pair is more inert than stereoactive.

respectively. Values greater than 0.05 valence units (vu) indicate that the structure is strained, whereas values greater than 0.20 vu indicate strain so great that the structure is unstable. For all of the reported materials, GII > BSI, indicating that the lattice-induced strains are greater than those attributable to electronic distortions (i.e., SOJT effects) (see Table 3).[53] Interestingly, for the polar materials, the BSI and GII values are approximately equal to or smaller than the corresponding values for the nonpolar materials (see Table 3). SOJT effects occur for the Ti^{4+} and I^{5+} cations but are observed structurally only for the latter. As we noted previously,[54] in oxides containing octahedrally coordinated d^0 cations linked to lone-pair polyhedra, the SOJT distortion associated with the d^0 cation is in a direction *away* from the oxide ligand bridging the two metal ions (i.e., the d^0 metal and lone-pair cation). In all of the materials reported here, the Ti^{4+} ion is completely surrounded by six IO_3 groups, effectively "trapping" the Ti^{4+} cation in the center of its oxide octahedron. As a result of this trapping, the magnitude of the Ti^{4+} distortion is effectively zero. We were able to calculate this magnitude using continuous-symmetry measures.[55−57] For $Li_2Ti(IO_3)_6$ and $Na_2Ti(IO_3)_6$, the magnitudes are 3.8×10^{-4} and 1.4×10^{-4} Å^2, respectively,[58] whereas for $A_2Ti(IO_3)_6$ (A = K, Rb, Cs, Tl), the distortion magnitudes are exactly zero since all six Ti−O bonds are identical. All of the distortion magnitudes are substantially smaller than the average magnitude for Ti^{4+} (∼0.056 Å^2).[54]

Infrared Spectroscopy. The IR spectra of all of the reported iodates reveal Ti−O vibrations at ∼630−680 cm^{-1}. Additional stretches at 760−830 and 430−500 cm^{-1} can be attributed to I−O vibrations. The IR spectra and assignments are given in Figure S8 in the Supporting Information.

UV−Vis Diffuse Reflectance Spectroscopy. UV−vis diffuse reflectance spectra were collected on all the reported iodates (see Figure S9 in the Supporting Information). Absorption (*K*/*S*) data were calculated from the following Kubelka−Munk function:[38,39]

$$F(R) = \frac{(1-R)^2}{2R} = \frac{K}{S}$$

where *R* is the reflectance, *K* the absorption, and *S* the scattering. In the (*K*/*S*)-versus-*E* plots, extrapolating the linear part of the rising curve to zero provided the onset of absorption at ∼3.3 eV for $Na_2Ti(IO_3)_6$, $K_2Ti(IO_3)_6$, $Rb_2Ti(IO_3)_6$, $Cs_2Ti(IO_3)_6$, and $Tl_2Ti(IO_3)_6$. The band gap for each material is attributable to the interaction of the Ti−O and I−O bonds, consistent with our first-principles calculations (see the Calculations section).

Thermogravimetric Analysis. TGA measurements revealed that all of the reported materials decompose above 400 °C. Powder XRD of the decomposition products revealed mixtures of mixed-metal titanates, alkali-metal iodides, and titanium dioxide. The TGA data are shown in Figure S10 in the Supporting Information.

Ion-Exchange Reactions. As all of the materials are zero-dimensional, we thought it would be possible to subject the alkali-metal cations to ion exchange. Attempts to exchange the Na^+ in $Na_2Ti(IO_3)_6$ with Li^+ by using excess LiCl(aq) at room temperature for 24 h produced a white powder that was subsequently shown to be unexchanged $Na_2Ti(IO_3)_6$. Ion-exchange reactions performed at 60 °C for 12 h resulted in decomposition of $Na_2Ti(IO_3)_6$ to TiO_2. Similar results were obtained in the ion-exchange reactions of $Cs_2Ti(IO_3)_6$ with K^+ and Rb^+.

Functional Inorganic Properties: Second-Harmonic Generation, Piezoelectricity, and Polarization. As $Li_2Ti(IO_3)_6$ and $Na_2Ti(IO_3)_6$ are NCS polar, we investigated their SHG, piezoelectric, and polarization properties (see Table 3). Since the two materials are isostructural, it is not surprising that the magnitudes of the aforementioned properties are very similar. The SHG efficiencies of both materials are very strong, ∼500 and ∼400 times that of α-SiO_2 for $Li_2Ti(IO_3)_6$ and $Na_2Ti(IO_3)_6$, respectively. The efficiencies compare well to $BaTiO_3$ and $LiNbO_3$ (400 and 600 times that of α-SiO_2, respectively).[40] The strong efficiencies are attributable to the parallel alignment of the local dipole moments in the IO_3 polyhedra (see Figure 2). Additional SHG measurements indicated that both materials are phase-matchable (see Figure S11 in the Supporting Information), with $\langle d_{eff} \rangle$ values of 26 and 23 pm/V for $Li_2Ti(IO_3)_6$ and $Na_2Ti(IO_3)_6$, respectively. Converse piezoelectric measurements were also

(53) Brown, I. D. *The Chemical Bond in Inorganic Chemistry: The Bond Valence Model*, 1st ed.; Oxford University Press: Oxford, U.K., 2002.
(54) Halasyamani, P. S. *Chem. Mater.* **2004**, *16*, 3586.
(55) Zabrodsky, H.; Peleg, S.; Avnir, D. *J. Am. Chem. Soc.* **1992**, *114*, 7843.
(56) Alvarez, S.; Avnir, D.; Llunell, M.; Pinsky, M. *New J. Chem.* **2002**, *26*, 996.
(57) Alvarez, S.; Alemany, P.; Casanova, D.; Cirera, J.; Llunell, M.; Avnir, D. *Coord. Chem. Rev.* **2005**, *249*, 1693.
(58) Llunell, M.; Casanova, D.; Cirera, J.; Bofill, J. M.; Alemany, P.; Alvarez, S.; Pinsky, M.; Avnir, D. *Shape Program*, version 1.1b; University of Barcelona: Barcelona, Spain, 2004.

Table 3. BVS, BSI, and GII Values, Dipole Moments, Magnitudes of Ti^{4+} Distortion (Å^2), SHG Efficiencies (Relative to α-SiO_2), Piezoelectric Responses, Pyroelectric Coefficients, and Maximum Polarizations for $A_2Ti(IO_3)_6$ (A = Li, Na, K, Rb, Cs, Tl)

	BVS					dipole moment						
compound	A^+	Ti^{4+}	I^{5+}	BSI	GII	Ti^{4+}	I^{5+}	Ti^{4+} distortion (10^{-4} Å^2)	SHG efficiency	piezo. d_{33} (pm/V)	pyro. coeff. (55 °C, μC m^{-2} K^{-1})	max P (100 Hz)
$Li_2Ti(IO_3)_6$	0.91	4.18	4.94	0.026	0.118	0.29	14.42	3.8	500	81	−2.4	0.27
$Na_2Ti(IO_3)_6$	1.21	4.09	5.04	0.016	0.102	0.16	14.20	1.4	400	60	−0.8	0.16
$K_2Ti(IO_3)_6$	1.05	4.10	4.89	0.044	0.127	0	14.87	0	–	–	–	–
$Rb_2Ti(IO_3)_6$	1.03	3.97	5.09	0.042	0.113	0	15.83	0	–	–	–	–
$Cs_2Ti(IO_3)_6$	1.11	4.11	5.03	0.044	0.151	0	14.94	0	–	–	–	–
$Tl_2Ti(IO_3)_6$	1.08	4.23	4.86	0.046	0.178	0	14.50	0	–	–	–	–

performed and revealed d_{33} values of 81 and 60 pm/V for $Li_2Ti(IO_3)_6$ and $Na_2Ti(IO_3)_6$, respectively (see Figure S12 in the Supporting Information). These charge constants compare well to those for other iodates, i.e., $LiIO_3$ (d_{33} = 92 pm/V) and KIO_3 (d_{33} = 39 pm/V).[59,60] Since both materials are polar, ferroelectric and pyroelectric measurements were performed. Although ferroelectric "loops" were observed in the ferroelectric measurements,, the materials are *not* ferroelectric. The loops are attributable to dielectric loss and not ferroelectric hysteresis (see Figure S13 in the Supporting Information).[61] In other words, the macroscopic polarization cannot be reversed (or switched) in the presence of an external electric field. Macroscopic polarization reversal implies microscopic polarization reversal, i.e., the local polarization associated with Ti^{4+} and I^{5+} must be reversed, or at a minimum reoriented, in the presence of an external electric field. The distortion associated with Ti^{4+} is effectively zero, and thus, the magnitude of its polarization is negligible (see Table 3). This is not the case with I^{5+}. The IO_3 polyhedron exhibits a substantial polarization in the direction opposite the lone pair. It is this polarization that must be switched, or at least reoriented, in order for $Li_2Ti(IO_3)_6$ and $Na_2Ti(IO_3)_6$ to be ferroelectric. As we will demonstrate in the Calculations section, IO_3 polyhedral polarization reversal is energetically very unfavorable. Pyroelectric measurements revealed pyroelectric coefficients of −2.4 and −0.8 μC m^{-2} K^{-1} for $Li_2Ti(IO_3)_6$ and $Na_2Ti(IO_3)_6$, respectively. These values are consistent with those for polar materials that are not ferroelectric, such as ZnO (−9.4 μC m^{-2} K^{-1}) and tourmaline (−4.0 μC m^{-2} K^{-1}).[62]

Calculations. Electronic structure calculations on $Na_2Ti(IO_3)_6$, $K_2Ti(IO_3)_6$, and $Tl_2Ti(IO_3)_6$ were performed in order to examine their band structures as well as to better understand the lone pairs associated with I^{5+} and Tl^+. The electronic band structures of $Na_2Ti(IO_3)_6$, $K_2Ti(IO_3)_6$, and $Tl_2Ti(IO_3)_6$ were determined using pseudopotential calculations. The electronic structures (see Figure S14 in the Supporting Information) show energy gaps of ∼2.95, 3.14, and 2.88 eV at the Fermi level (E_F) for $Na_2Ti(IO_3)_6$, $K_2Ti(IO_3)_6$, and $Tl_2Ti(IO_3)_6$, respectively.[32] The energy gaps are consistent with those experimentally observed in the UV−vis diffuse reflectance spectra. From the total and projected density of states analyses, three valence bands are exhibited, one each in the lower, middle, and upper energy regions below the Fermi level. In the lower and middle regions, the energy bands are composed mostly of I 5s and O 2s orbitals and I 5p and O 2p orbitals, respectively. In the upper region, the bands are made up mainly of O 2p orbitals. Also, the bottoms of their conduction bands have significant Ti 3d and I 5p orbital contributions. In spite of the different crystal symmetries, the valence bands have similar orbital contributions because of the similarities in the structural topologies, i.e., zero-dimensional features with nearly equivalent local coordination environments for the Ti^{4+} and I^{5+} cations.

The visualizations of the electron localization functions (ELFs)[63,64] for the polar and nonpolar compounds clearly indicate how the local polarizations result in a macroscopic dipole moment (Figure 2) or in complete cancellation (Figure 3). Figures 2 and 3 show the ELF isosurfaces with η = 0.9 calculated using norm-conserving MT pseudopotential methods. Both figures clearly show a lobelike isosurface near each I^{5+} cation that may be considered as a stereoactive lone pair. The lone pairs on $Na_2Ti(IO_3)_6$ (see Figure 2) are aligned in a parallel manner, resulting in a macroscopic dipole moment and thus rendering the material polar, whereas in $K_2Ti(IO_3)_6$ and $Tl_2Ti(IO_3)_6$ (see Figure 3), the lone pairs are pointed in opposite directions, resulting in a CS nonpolar material. Interestingly, in $Tl_2Ti(IO_3)_6$, a spherelike isosurface around Tl^+ is observed, indicating that the lone pair is more inert than stereoactive.

The question of why $Li_2Ti(IO_3)_6$ and $Na_2Ti(IO_3)_6$, although polar, are *not* ferroelectric is very relevant. As we stated earlier, our ferroelectric measurements indicate that the observed loops are attributable to dielectric loss and not polarization reversal. For polarization reversal, the six IO_3 polyhedra must invert (we are assuming that the polarization attributable to Ti^{4+} is negligible). One "mechanism" for polarization reversal would be an umbrella-type inversion of the IO_3 polyhedron analogous to that of NH_3. A second possible "mechanism" would involve complete rotation of the IO_3 polyhedron, akin to that of the NO_2 molecule in ferroelectric $NaNO_2$.[2] Our calculations show that in $Na_2Ti(IO_3)_6$, the former is energetically unfavorable whereas the latter would require large movements of the stereoactive lone pairs in the structure. It should also be noted that NH_3 and $NaNO_2$ are molecular compounds, whereas $Li_2Ti(IO_3)_6$ and $Na_2Ti(IO_3)_6$ are solid-state materials with extended bond networks. To evaluate how the total energy would vary during the hypothetical polarization reversal (i.e., the umbrella-type reversal), we performed frozen phonon calculations in which the I^{5+} cation was displaced along the pseudo-threefold axis in the IO_3 polyhedron (see Figure 4). In Figure 4, movement of the I^{5+} cation away from its original position toward the base of the IO_3 polyhedron is in the $+l$ direction, whereas the opposite displacement is in the $-l$ direction. The calculations were performed for all six IO_3 polyhedra that are bonded to a TiO_6 octahedron and then normalized for one IO_3 polyhedron. Figure

(59) Hamid, S. A. *Phys. Status Solidi A* **1977**, *43*, K29.
(60) Landolt, H., *Numerical Values and Functions from the Natural Sciences and Technology (New Series), Group 3: Crystal and Solid State Physics*; Springer Verlag: Berlin, 1979; Vol. 11, p 317.
(61) Scott, J. F. *J. Phys.: Condens. Matter* **2008**, *20*, 021001.
(62) Lang, S. B. *Phys. Today* **2005**, *58*, 31.
(63) Becke, A. D.; Edgecombe, K. E. *J. Chem. Phys.* **1990**, *92*, 5397.
(64) Savin, A.; Jepsen, O.; Flad, J.; Andersen, O. K.; Preuss, H.; Von Schnering, H. G. *Angew. Chem.* **1992**, *104*, 186; *Angew. Chem., Int. Ed. Engl.* **1992**, *31*, 187.

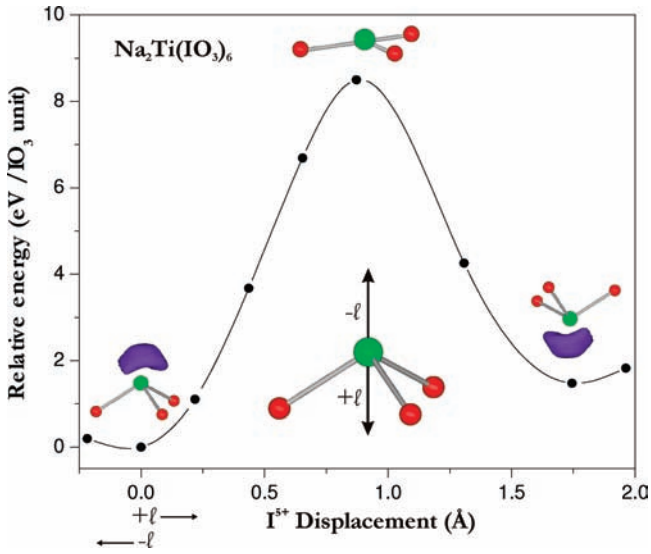

Figure 4. Energy landscape with respect to the I^{5+} displacement for the inversion of the IO_3 polyhedra. The calculations (●) were performed with the I^{5+} cation moving in the $+l$ direction as defined in the text. The energy barrier to inversion is ~8.5 eV.

4 depicts the energy landscape (i.e., the relative energy per IO_3 polyhedron) with respect to the I^{5+} displacement. Clearly, two energy minima and one maximum are observed. The two minima correspond to the relative energies of the original and inverted IO_3 polyhedron. It is interesting to note that the energy of the inverted IO_3 polyhedron is higher than the original. In the hypothetical inverted structure, the I^{5+} and Ti^{4+} cations are closer to each other, resulting in energetically unfavorable interactions that raise the energy. The maximum corresponds to the energy barrier to inversion (see Figure 4), which is very large (~8.5 eV). Comparing this value with those for well-known ferroelectrics such as $BaTiO_3$ (~1.8×10^{-2} eV) and $PbTiO_3$ (~2.0×10^{-1} eV)[65] clearly demonstrates why $Na_2Ti(IO_3)_6$ is not ferroelectric: polarization reversal of the IO_3 polyhedra is energetically very unfavorable (i.e., nearly 500 and 45 times the energy required for $BaTiO_3$ and $PbTiO_3$, respectively). On the basis of these calculations, it is not unreasonable to suggest that in oxides, other fifth-period lone-pair cations (e.g., Sn^{2+}, Sb^{3+}, and Te^{4+}) will have similar energy barriers and thus will *not* undergo polarization reversal.

NCS Polar versus CS Nonpolar Structures. One of the most interesting features about the reported series of materials is that there is a change in macroscopic polarity from NCS polar to CS nonpolar as we progress from the smaller cations, Li^+ and Na^+, to the larger ones, K^+, Rb^+, Cs^+, and Tl^+. It was mentioned earlier that all six materials exhibit a zero-dimensional structural topology consisting of a TiO_6 octahedron surrounded by six IO_3 polyhedra, i.e., a $\{[TiO_{6/2}]^{2-}\cdot 6[IO_{1/2}O_{2/1}]^0\}^{2-}$ anion. These anions pack around the alkali-metal or Tl^+ cations. For macroscopic, crystallographic polarity to occur, two requirements must be met. First, local polarity must be present: some of the local coordination polyhedra must exhibit a dipole moment. Second, some of the local polarizations must "constructively add" to create a crystallographically polar material. Very often, the first condition is met but the local moments point in opposite directions, resulting in a CS nonpolar material. For the reported materials,

(65) Cohen, R. E. *Nature* **1992**, *358*, 136.

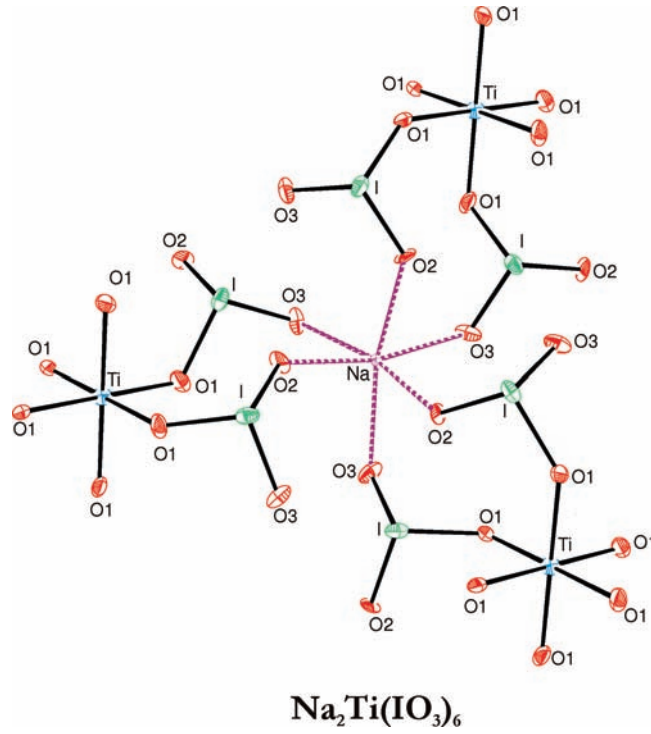

Figure 5. ORTEP diagram (with 50% probability ellipsoids) for $Na_2Ti(IO_3)_6$, with the Na^+ coordination environment emphasized (dashed purple bonds). It should be noted that the Na^+ cation makes an oxide bond with each of six IO_3 polyhedra.

the local polarity is attributable solely to the IO_3 polyhedra, since the polarization associated with the TiO_6 octahedron is negligible (Li and Na phases) or zero (K, Rb, Cs, and Tl phases) (see Table 3). NCS polar structures are observed for the smaller cations, Li^+ and Na^+, whereas CS nonpolar structures are found for the larger ones, K^+, Rb^+, Cs^+, and Tl^+. Because of the ionic size of Li^+ and Na^+, (relatively) small coordination environments are preferred. In $Li_2Ti(IO_3)_6$ and $Na_2Ti(IO_3)_6$, the Li^+ and Na^+ cations are in pseudo-octahedral coordination environments and interact with oxide ligands on six different IO_3 polyhedra (see Figure 5). To create this octahedral environment around each of the Li^+ and Na^+ cations, the IO_3 polyhedra must be aligned in a parallel manner around the Ti^{4+} cation. This parallel alignment results in a macroscopically polar material, i.e., the second condition mentioned above is fulfilled. It may seem structurally possible for the IO_3 polyhedra to arrange themselves around Ti^{4+} in an antiparallel manner, with the lone-pair direction alternating between "up" and "down", while still retaining pseudo-octahedral coordination environments for Li^+ and Na^+. A ball-and-stick representation of this hypothetical structure is shown in Figure 6. The hypothetical structure shows that six-coordinate Li^+ and Na^+ is still viable. However, if the IO_3 polyhedra were to be arranged in an antiparallel manner, unfavorable lone-pair−lone-pair interactions would occur *between* the $\{[TiO_{6/2}]^{2-}\cdot 6[IO_{1/2}O_{2/1}]^0\}^{2-}$ anions. These unfavorable interactions are indicated by yellow shaded circles in Figure 6. Thus, an antiparallel arrangement of IO_3 polyhedra is not structurally possible, even if Li^+ and Na^+ retain pseudo-octahedral coordination environments.

For the CS nonpolar materials, a different situation occurs. The large ionic sizes of K^+, Rb^+, Cs^+, and Tl^+ require larger coordination environments. In $A_2Ti(IO_3)_6$ (A = K, Rb, Cs, Tl), the A^+ cations are in ninefold coordination environments (see Figures S3−S6 in the Supporting Information). The larger

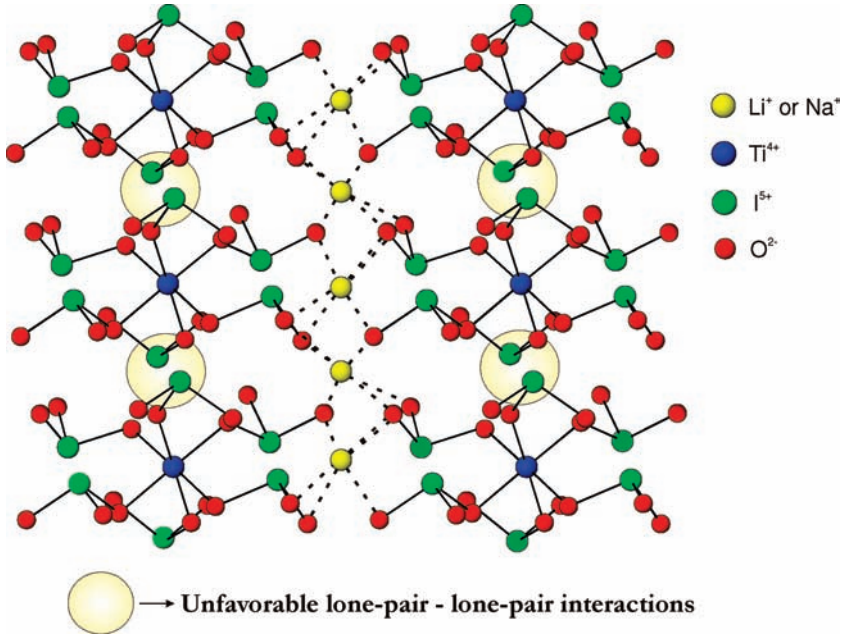

Figure 6. Hypothetical ball-and-stick representation of $A_2Ti(IO_3)_6$ (A = Li, Na) in which the IO_3 polyhedra are antiparallel. In this representation, the A^+ cations remain six-coordinate, but there are unfavorable interactions between the IO_3 lone pairs. These are highlighted by yellow circles.

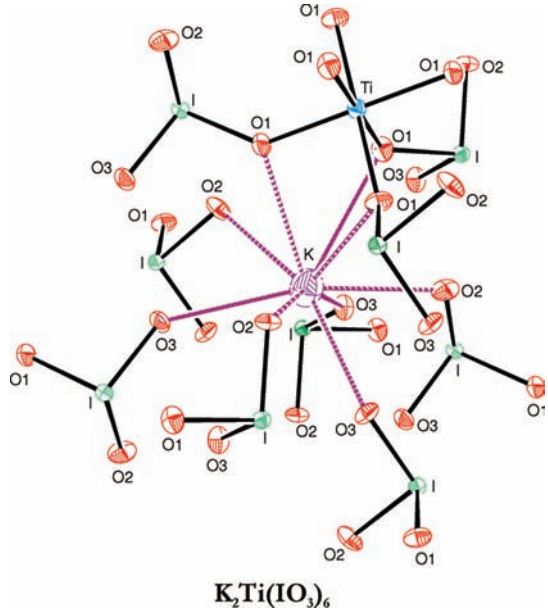

Figure 7. ORTEP diagram (with 50% probability ellipsoids) for $K_2Ti(IO_3)_6$, with the K^+ coordination environment emphasized (dashed purple bonds). It should be noted that the K^+ cation makes nine oxide bonds with nine IO_3 polyhedra and a TiO_6 octahedron.

cations interact with oxide ligands on nine different IO_3 groups and a TiO_6 octahedron (see Figure 7). In fact, three of the oxide ligand contacts are bonded to both Ti^{4+} and I^{5+} cations. Structurally, the only manner in which the larger A^+ cations can have nine oxide contacts, involving both TiO_6 and IO_3 polyhedra, is for the IO_3 polyhedra to rotate with respect to the Ti^{4+} cation. This rotation has two consequences. First, the local IO_3 dipole moments point in equal and opposite directions, rendering the material CS nonpolar (see Figure 3). Second, the rotation allows the larger A^+ cations access to oxide ligands that are bonded to both Ti^{4+} and I^{5+} cations (see Figure 7). This rotation is not necessary for the smaller cations, Li^+ and Na^+, as six Li−O (Na−O) contacts can be fully achieved by six IO_3 polyhedra. Bond valence calculations support our argument. When we replaced Li^+ in the $Li_2Ti(IO_3)_6$ structure with K^+, Rb^+, Cs^+, and Tl^+ and calculated the bond valence sums for the larger cations, we obtained values of 5.23, 4.80, 8.35, and 5.38, respectively, whereas for Li^+, the value is 0.91 (see Table 4). Clearly, in the smaller coordination environment, the larger cations are severely overbonded. Conversely, when we replaced K^+ in the $K_2Ti(IO_3)_6$ structure with Li^+ and Na^+ and calculated the bond valence sums for the smaller cations, we obtained values of 5.69 and 7.60, respectively, whereas for K^+, the value is 1.05. The large coordination environments for the smaller cations also result in substantial overbonding. Thus, it is the A^+ cation size, the corresponding coordination environment preference, and bond valence requirements that determine the macroscopic polarity of the material.

Table 4. BVS Values for (a) K^+, Rb^+, Cs^+, and Tl^+ Cations in the $Li_2Ti(IO_3)_6$ Structure and (b) Li^+ and Na^+ Cations in the $K_2Ti(IO_3)_6$ Structure

		(a) $Li_2Ti(IO_3)_6$			
cation	Li^+	K^+	Rb^+	Cs^+	Tl^+
BVS	0.91	5.23	4.80	8.35	5.38
		(b) $K_2Ti(IO_3)_6$			
cation	K^+		Li^+	Na^+	
BVS	1.05		5.67	7.60	

Conclusions

We have demonstrated that in the $A_2Ti(IO_3)_6$ (A = Li, Na, K, Rb, Cs, Tl) system, the macroscopic polarity is controlled by the A^+ cation. The materials with smaller cations, Li^+ and Na^+, are noncentrosymmetric and polar, whereas compounds with the larger cations, K^+, Rb^+, Cs^+, and Tl^+, are centrosymmetric and nonpolar. The smaller cations are in pseudo-octahedral coordination environments and interact with six oxide ligands on six different IO_3 polyhedra. These interactions require the IO_3 polyhedra to align in a parallel manner, rendering $Li_2Ti(IO_3)_6$ and $Na_2Ti(IO_3)_6$ NCS and polar. The larger cations, K, Rb, Cs and Tl, are in ninefold coordinate environments and

interact with oxide ligands on both IO_3 and TiO_6 polyhedra. In order for these interactions to take place, the IO_3 polyhedra must rotate with respect to the TiO_6 octahedron. This rotation aligns the IO_3 polarizations in opposite directions, rendering all four of the materials $K_2Ti(IO_3)_6$, $Rb_2Ti(IO_3)_6$, $Cs_2Ti(IO_3)_6$, and $Tl_2Ti(IO_3)_6$ CS nonpolar. Although $Li_2Ti(IO_3)_6$ and $Na_2Ti(IO_3)_6$ are polar, the materials are not ferroelectric. In other words, the polarization cannot be reversed, or reoriented, in the presence of an external electric field. Our calculations have demonstrated that reversing the polarization on the IO_3 polyhedra is energetically unfavorable.

Acknowledgment. H.-Y.C., S.-H.K., and P.S.H. thank the Welch Foundation, NSF (DMR-0652150), and ACS PRF (47345-AC10) for support. K.M.O. thanks KOSEF for financial support through the Nuclear R&D 3N Researcher Program (2008-03981).

Supporting Information Available: Additional experimental and theoretical data (PDF, XLS, CIF). This material is available free of charge via the Internet at http://pubs.acs.org.

JA9015099